Downloaded from www.ajronline.org by Lund University Medicinska Fakultetens Bibl. on 09/02/17 from IP address 130.235.66.10. Copyright ARRS. For personal use only; all rights reserved

Detection of Myocardial Infarction Using Delayed Enhancement Dual-Energy CT in Stable Patients

Gaston A. Rodriguez-Granillo[1]
Roxana Campisi
Alejandro Deviggiano
Maria N. Lopez de Munain
Macarena De Zan
Carlos Capunay
Patricia Carrascosa

OBJECTIVE. The objective of our study was to explore whether delayed enhancement dual-energy CT (DECT) allows the detection of myocardial infarcts in stable patients.

SUBJECTS AND METHODS. Patients with known or suspected coronary artery disease clinically referred for myocardial perfusion imaging using SPECT were prospectively included. All patients ($n = 34$) also underwent stress, rest, and delayed enhancement DECT on a DECT scanner. At SPECT, segments with myocardial infarction (MI) were defined as those with a summed rest score of ≥ 2 in two or more consecutive segments, and a diagnosis of MI was supported by wall motion abnormalities, clinical history, and ECG findings.

RESULTS. Segments with MI were identified in 13 (38%), 15 (44%), and 14 (41%) patients using SPECT, perfusion CT, and delayed enhancement DECT, respectively. When combined SPECT and perfusion CT results were used as the reference standard, delayed enhancement DECT had a sensitivity, specificity, positive predictive value, and negative predictive value for the detection of MI of 91.7% (95% CI, 62–98%), 86.4% (95% CI, 65–97%), 78.6% (95% CI, 49–95%), and 95.0% (95% CI, 75–100%). At delayed enhancement DECT (40 keV), a signal attenuation higher than 161 HU had a sensitivity of 72% and a specificity of 79% for the detection of MI on a per-segment basis. The median signal attenuation of myocardial infarcts at 40 keV was 3.0 SDs (interquartile range, 1.3–4.0 SDs) above that of normal myocardium.

CONCLUSION. In this study, delayed enhancement DECT allowed the detection of myocardial infarcts in stable patients.

Keywords: chronic myocardial infarction, delayed enhancement, fibrosis, late enhancement, spectral imaging

DOI:10.2214/AJR.17.18118

Received February 17, 2017; accepted after revision April 9, 2017.

P. Carrascosa is a consultant to GE Healthcare.

[1]All authors: Department of Cardiovascular Imaging, Diagnóstico Maipú, Avenue Maipu 1668, Buenos Aires B1602BQ, Argentina. Address correspondence to G. A. Rodriguez-Granillo (grodriguezgranillo@gmail.com).

AJR 2017; 209:1–10

0361–803X/17/2095–1

© American Roentgen Ray Society

Although cardiac CT was originally conceived and validated as an accurate noninvasive diagnostic tool for the assessment of coronary atherosclerosis, it has evolved during the past decade to comprise several noncoronary applications. Iodinated and gadolinium-derived contrast media have similar kinetics, leading to comparable myocardium perfusion and infarct imaging using both MRI and CT [1–3]. This has positioned cardiac CT as a potential one-stop-shop tool for the comprehensive assessment of patients with suspected or established coronary artery disease (CAD) because it can be used to evaluate the coronary anatomy, determine the functional significance of findings, and characterize infarct in a single session [4, 5]. Nonetheless, with the exception of the acute myocardial infarction (MI) setting in which membrane disruption leads to significant extracellular volume expansion, cardiac CT suffers from limited contrast tissue resolution compared with cardiac MRI [4, 6, 7]. This lower resolution of CT has led to suboptimal results in the assessment of patients with chronic MI, with low sensitivities reported for the detection of patients with ischemic scar even when using newer-generation scanners [1, 4, 5, 8].

Virtual monochromatic imaging (VMI) derived from dual-energy CT (DECT) has emerged as a tool with the ability to minimize beam-hardening artifacts and thus improve the diagnostic performance of pharmacologic stress perfusion CT [9]. In addition, higher intravascular attenuation levels can be obtained by low-energy monochromatic imaging [10]. This has allowed a significant reduction in the iodinated contrast load required for cardiac CT, and in the setting of delayed enhancement, DECT shows promise for improving the identification of fibrotic areas [11].

We therefore sought to explore whether VMI at low energy levels derived from delayed enhancement DECT allows the detection of myocardial infarcts in stable patients.

Downloaded from www.ajronline.org by Lund University Medicinska Fakultetens Bibl. on 09/02/17 from IP address 130.235.66.10. Copyright ARRS. For personal use only; all rights reserved

Materials and Methods

Patients with known or suspected CAD clinically referred for myocardial perfusion imaging using SPECT were prospectively included. Patients with a low or low-to-intermediate probability of CAD were excluded. Data regarding stress and rest myocardial perfusion CT of a subset of these patients have been previously published [9], whereas the delayed enhancement DECT data have never been reported. All patients included in the study were in sinus rhythm; able to maintain a breath-hold for at least 10 seconds; and did not have a history of contrast-related allergy, renal failure, or hemodynamic instability. Patients younger than 18 years old and patients with a body mass index (BMI [weight in kilograms divided by the square of height in meters]) greater than 32, unstable angina, a history of MI within the previous 30 days, a history of a percutaneous coronary revascularization procedure within the previous 6 months, chronic heart failure, chronic obstructive pulmonary disease, or a high-degree atrioventricular block, were excluded. For the 24 hours before imaging, vasodilator drugs were withdrawn and patients were advised to avoid smoking and caffeinated beverages.

The protocol of this study was approved by the institutional ethics committee, and all examinations were performed in accordance with the ethical standards as described in the 1964 Declaration of Helsinki and its later amendments. Informed consent was obtained from all participants included in the study.

Dual-Energy CT Acquisition

All patients were scanned on a single-source DECT scanner using rapid switching (0.3–0.5 ms) between low (80 kV) and high (140 kV) tube potentials (Discovery HD 750, GE Healthcare) to enable the reconstruction of low- and high-energy projections and the generation of VMI reconstructions in 10-keV increments ranging from 40 to 140 keV. Iterative reconstruction was applied at 40% adaptive statistical iterative reconstruction (ASiR 40, GE Healthcare) from 60 to 140 keV, because 60 keV is the lowest monoenergetic level available for this purpose in our software version.

All patients underwent the following examinations: first, stress imaging (contrast-enhanced); second, rest imaging (contrast-enhanced, 30 minutes after stress); and, third, delayed enhancement DECT (unenhanced). The administration of iodinated contrast material (iobitridol [Xenetix 350, Guerbet]) was performed using a dual-phase protocol with 50–70 mL, according to the BMI, and was followed by a 30- to 40-mL saline flush at stress and rest imaging. Stress imaging was performed using dipyridamole (0.56 mg/kg) administered over the course of 4 minutes. After rest imaging, a 30- to 40-mL additional dose of contrast medium was administered, and delayed enhancement DECT images were obtained 10 minutes later. All acquisitions were executed using prospective ECG-gating including 150–200 ms of temporal padding aimed to cover approximately 40–75% of the cardiac cycle for stress acquisitions, 100-ms padding centered at 75% of the cardiac cycle for rest scans, and no padding at 75% for delayed enhancement DECT scans. For rest imaging, patients with a heart rate greater than 65 beats/min received 5 mg of IV propranolol if needed to achieve a target heart rate of less than 60 beats/min, and image acquisition was executed after sublingual administration of 2.5–5 mg of isosorbide dinitrate. A bolus-tracking technique was used to synchronize the arrival of contrast material at the level of the coronary arteries with the start of scanning.

The same pharmacologic stress infusion was used for stress perfusion CT and SPECT. Dipyridamole and iodinated contrast material were administered using two independent antecubital IV lines. After dipyridamole infusion, aminophylline (1–2 mg/kg) was given IV to revert the vasodilator effect.

Myocardial Perfusion Imaging Using SPECT

Myocardial perfusion imaging using SPECT was performed using a previously described 2-day gated stress-rest protocol [12]. At the time of stress perfusion CT, 2 minutes after dipyridamole administration and immediately before the perfusion CT scans were obtained, 10–15 mCi of ^{99m}Tc-methoxyisobutylisonitrile (MIBI) was administered. Stress SPECT image acquisition was performed 60 minutes after the administration of the radiotracer using a dual-head gamma camera over a 90° circular orbit (Millennium MG, GE Healthcare). Data were acquired in a 128 × 128 matrix for 32 projections in a step-and-shoot format. Rest SPECT image acquisition was completed within 24–48 hours after stress SPECT after the administration of 10–15 mCi of ^{99m}Tc-MIBI.

Dual-Energy CT and SPECT Analyses

Stress and rest perfusion CT images were analyzed by an observer with experience in perfusion CT using a smooth filter in the axial planes and multiplanar reconstructions. Evaluation of ventricular segments was performed using the American Heart Association's 17-segment model, and segment 17 (i.e., the apex) was excluded [13]. Short-axis views were obtained initially using 5- to 8-mm average multiplanar reconstructions from the base to the apex. Images were analyzed using VMI data in gray-scale. Different energy levels from 40 to 140 keV were applied to confirm or to rule out the presence of a perfusion defect, and findings were considered positive only if identified at 40–100 keV. Myocardial perfusion defects were detected in a qualitative manner on the basis of signal attenuation and were compared with the signal attenuation assessed over a normally perfused segment [9]. Reduced wall thickness of the underlying myocardium, if present, was used as support for the diagnosis of myocardial infarcts (Fig. 1).

Analysis of delayed enhancement DECT studies was performed by a second observer with experience in delayed enhancement DECT who was blinded to clinical history, ECG findings, and results of perfusion CT and SPECT. The delayed enhancement DECT images were evaluated at all available energy levels (40–140 keV) using short-axis views with 7.3-mm average multiplanar reconstructions. Window width and level were adjusted at the observer's discretion for every energy level assessed. The presence of late iodine enhancement (myocardial infarcts) was defined visually as myocardial areas with a focal increase of signal attenuation compared with that of the remote normal myocardium, concordant with interruption of the underlying nonenhanced (normal) myocardium or diminishing of the nonenhanced (epicardial) myocardial thickness (Figs. 1 and 2). The same observer reanalyzed the delayed enhancement DECT dataset 60 days later at the same energy levels for an analysis of intraobserver agreement.

SPECT analysis was carried out by consensus interpretation of myocardial perfusion data with visual overreading by two experienced observers who were blinded to the perfusion CT and delayed enhancement DECT data. Semiquantitative analysis was accomplished using the Cedars-Sinai method [14]. The summed rest score (SRS) was calculated. Myocardial infarction was determined on the basis of the resting images and was defined as an SRS of ≥ 2 in two or more consecutive segments of a corresponding coronary territory, and the diagnosis of MI was supported by findings on gated images aimed at the discrimination between true myocardial perfusion defects and attenuation artifacts. Clinical history and baseline ECG findings were available to the observers during SPECT analysis [15].

We evaluated the diagnostic performance of perfusion CT and delayed enhancement DECT for the detection of MI on a per-patient, per-territory, and per-segment basis using SPECT as the reference standard. Subsequently, using delayed enhancement DECT data, we identified left ventricular segments with MI identified at both perfusion CT and SPECT, and signal attenuation and image noise were determined with ROIs customized according to the size of the anatomic region at 40, 60, 80, 100, 120, and 140 keV (Fig. 3). Within the short-axis slice, signal attenuation and image noise were determined over areas with remote normal perfusion and a lack of late iodine enhancement. The signal attenuation of the left ventricular blood pool was also determined using standardized 300-mm^2 ROIs within the same short axis.

Downloaded from www.ajronline.org by Lund University Medicinska Fakultetens Bibl. on 09/02/17 from IP address 130.235.66.10. Copyright ARRS. For personal use only; all rights reserved

The effective radiation dose for CT was derived by multiplying the dose-length product by the weighting (k) value of 0.014 mSv/mGy·cm for chest examinations, as suggested by the Society of Cardiovascular Computed Tomography [16].

Statistical Analysis

Discrete variables are presented as counts and percentages. Continuous variables are presented as means ± SD, and variables with nonuniform distribution are presented as medians (interquartile range). Comparisons among groups were performed using paired-samples Student *t* tests and the one-way ANOVA. Nonparametric comparisons were performed using Wilcoxon signed-rank tests. The intraobserver variability was assessed

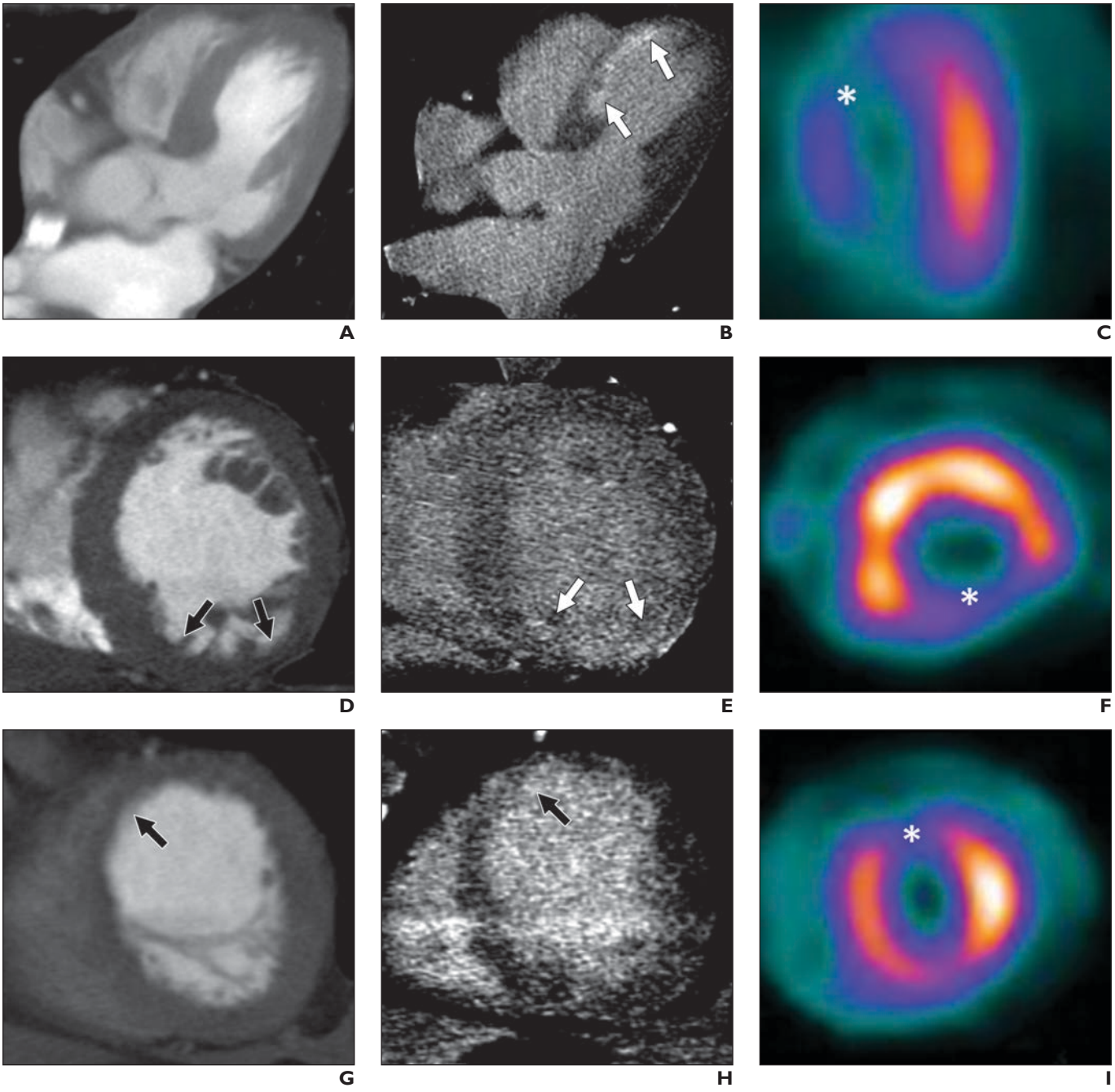

Fig. 1—Patients with myocardial infarct identified using delayed enhancement dual-energy CT (DECT), rest perfusion CT, and rest SPECT. It is noteworthy that infarcts are occasionally better portrayed using delayed enhancement DECT (at 40 keV) than rest perfusion CT—for example, **A–C**.
A–C, Rest perfusion CT (40 keV) (**A**), delayed enhancement DECT (**B**), and rest SPECT (**C**) images of 66-year-old man with body mass index (BMI [weight in kilograms divided by the square of height in meters]) of 29.4 show myocardial infarct (*arrows*, **B**; *asterisk*, **C**).
D–F, Rest perfusion CT (50 keV) (**D**), delayed enhancement DECT (**E**), and rest SPECT (**F**) images of 79-year-old man with BMI of 28.5 show myocardial infarct (*arrows*, **E**; *asterisk*, **F**).
G–I, Rest perfusion CT (40 keV) (**G**), delayed enhancement DECT (**H**), and rest SPECT (**I**) images of 66-year-old man with BMI of 28.3 show myocardial infarct (*arrows*, **G** and **H**; *asterisk*, **I**).

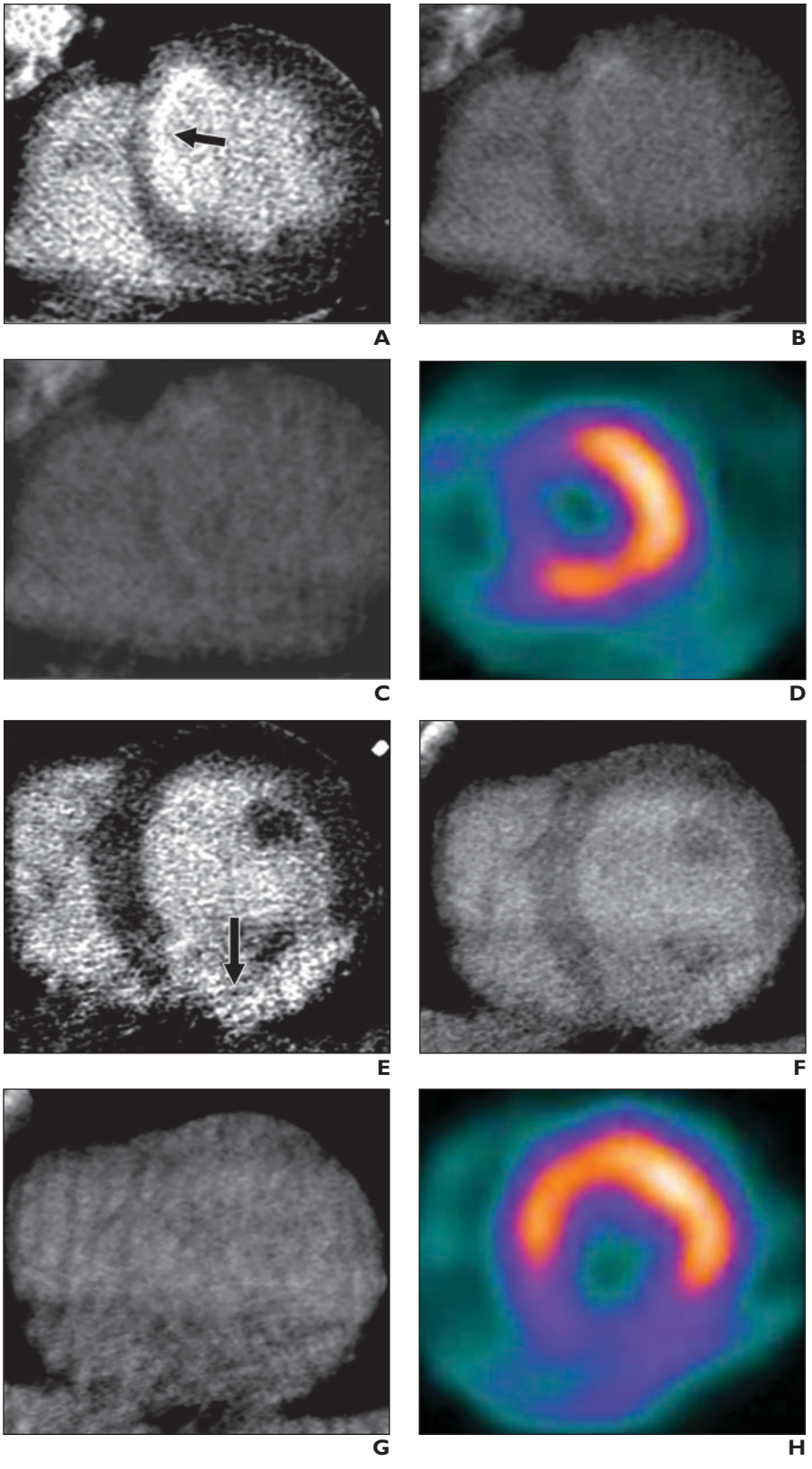

Fig. 2—Delayed enhancement dual-energy CT (DECT) images (midventricular short axis) obtained at different energy levels in three different patients with history of previous myocardial infarction (MI). Improved discrimination of MI is observed at lowest energy level. Short-axis SPECT images at rest depict severe perfusion defects, which is concordant with DECT findings.

A–D, Virtual monochromatic reconstruction delayed enhancement DECT images at 40 keV (**A**), 80 keV (**B**), and 140 keV (**C**) and short-axis rest SPECT image (**D**) of 68-year-old man with body mass index (BMI [weight in kilograms divided by the square of height in meters]) of 21.1 show MI (*arrow*, **A**).

E–H, Virtual monochromatic reconstruction delayed enhancement DECT images at 40 keV (**E**), 80 keV (**F**), and 140 keV (**G**) and short-axis rest SPECT image (**H**) of 46-year-old man with BMI of 29.0 show MI (*arrow*, **E**).

(Fig. 2 continues on next page)

Downloaded from www.ajronline.org by Lund University Medicinska Fakultetens Bibl. on 09/02/17 from IP address 130.235.66.10. Copyright ARRS. For personal use only; all rights reserved

Downloaded from www.ajronline.org by Lund University Medicinska Fakultetens Bibl. on 09/02/17 from IP address 130.235.66.10. Copyright ARRS. For personal use only; all rights reserved

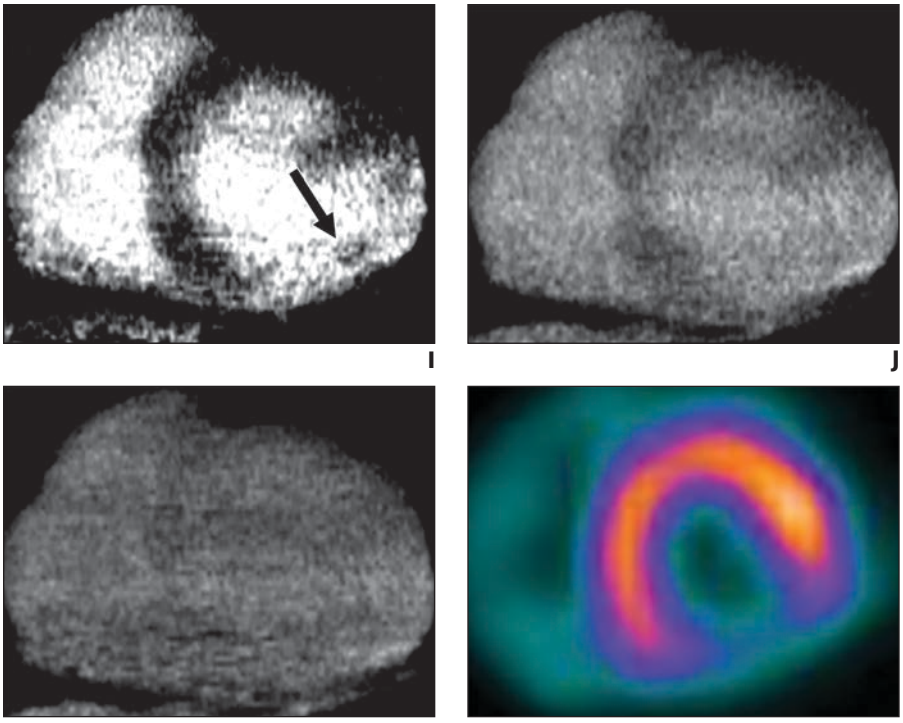

Fig. 2 (continued)—Delayed enhancement dual-energy CT (DECT) images (midventricular short axis) obtained at different energy levels in three different patients with history of previous myocardial infarction (MI). Improved discrimination of MI is observed at lowest energy level. Short-axis SPECT images at rest depict severe perfusion defects, which is concordant with DECT findings.
I–L, Virtual monochromatic reconstruction delayed enhancement DECT images at 40 keV (**I**), 80 keV (**J**), and 140 keV (**K**) and short-axis rest SPECT image (**L**) of 54-year-old man with BMI of 21.9 show MI (*arrow*, **I**).

TABLE 1: Characteristics of 34 Subjects and Effective Radiation Doses of Imaging Studies

Characteristic	Value
Age (y), mean ± SD	61.3 ± 11.4
Male	25 (74)
Diabetes	11 (32)
Hypercholesterolemia	26 (76)
Hypertension	28 (82)
Current smoker	6 (18)
Previous PCI	13 (38)
Body mass index[a], mean ± SD	27.9 ± 3.5
Effective radiation dose (mSv), mean ± SD	
Total	10.1 ± 1.6
Stress perfusion CT	4.7 ± 1.2
Rest perfusion CT	3.5 ± 0.8
Delayed enhancement dual-energy CT	2.2 ± 0.5

Note—Unless indicated otherwise, data are presented as number (%) of patients. PCI = percutaneous coronary intervention.
[a]Weight in kilograms divided by the square of height in meters.

using intraclass correlation coefficients (ICCs) (using a two-way random-effects model, absolute agreement, and average measurement) with 95% CIs. To determine the accuracy for the detection of MI, we calculated the sensitivity, specificity, positive predictive value (PPV), and negative predictive value (NPV) and performed ROC curve analyses accounting for potential nonuniform distribution (95% CIs). ROC curve analyses were performed using specific software for ROC analysis (MedCalc version 12.0, MedCalc Software). Pairwise comparisons of ROC curves were performed using the method of DeLong et al. [17] for the detection of differences between 2 AUCs, and we calculated the binomial exact CI for the AUC [17]. All other statistical analyses were performed using statistics software (SPSS for Windows, version 22.0, IBM). A two-sided p value of < 0.05 indicated statistical significance.

Results

Patient Population

Thirty-four patients were prospectively included in this study. The mean age was 61.3 ± 11.4 years, 25 (74%) were male, and 11 (32%) had diabetes; the mean BMI was 27.9 ± 3.5 (Table 1). Fourteen patients (41%) had a clinical history of previous MI. The mean effective radiation doses of stress perfusion CT, rest perfusion CT, and delayed enhancement DECT acquisitions are detailed in Table 1. Evidence of MI was identified in almost half of the patients (Table 2).

Diagnostic Performance of Delayed Enhancement Dual-Energy CT

All images of myocardial segments were considered of sufficient image quality for interpretation.

Using the combined SPECT and perfusion CT results as the reference standard, the sensitivity, specificity, PPV, and NPV of delayed enhancement DECT on a per-patient basis (91.7% [95% CI, 62–98%], 86.4% [95% CI, 65–97%], 78.6% [95% CI, 49–95%], 95.0% [95% CI, 75–100%]), per-territory basis (85.7% [95% CI, 57–98%], 96.6% [95% CI, 90–99%], 80.0% [95% CI, 52–96%], 97.7% [95% CI, 92–100%]), and per-segment basis (65.5% [95% CI, 51–78%], 96.3% [95% CI, 94–98%], 66.7% [95% CI, 53–79%], 96.1% [95% CI, 94–98%]) were similar to those when using only SPECT as the reference standard. The AUC of delayed enhancement DECT for the detection of MI was 0.89 (95% CI, 0.74–0.97) on a per-patient basis, 0.95 (95% CI, 0.89–0.98) on a per-

Downloaded from www.ajronline.org by Lund University Medicinska Fakultetens Bibl. on 09/02/17 from IP address 130.235.66.10. Copyright ARRS. For personal use only; all rights reserved

TABLE 2: Prevalence of Myocardial Infarction (MI) in 34 Study Subjects Based on Clinical History of MI, SPECT, Perfusion CT, and Delayed Enhancement Dual-Energy CT (DECT)

Clinical History or Imaging Modality	No. (%)			MI Localization (%)[a]		
	Per Patient	Per Territory	Per Segment	Anterior Wall	Lateral Wall	Inferior Wall
Clinical history of MI	14 (41)					
SPECT	13 (38)	14 (14)	70 (13)	43	29	29
Perfusion CT	15 (44)	16 (16)	77 (14)	38	25	38
Delayed enhancement DECT	14 (41)	15 (15)	54 (10)	47	27	27

[a]Percentages do not total 100 because of rounding.

territory basis, and 0.81 (95% CI, 0.77–0.84) on a per-segment basis.

Overall, segments with MI identified by both SPECT and perfusion CT showed significantly higher signal attenuation at delayed enhancement DECT (40-keV level) than segments with normal perfusion (mean ± SD, 186.3 ± 56.6 vs 136.2 ± 36.6 HU, respectively; $p < 0.0001$), as well as a higher signal-to-noise ratio (6.9 ± 3.8 vs 4.7 ± 2.3; $p < 0.0001$) and similar image noise (31.5 ± 12.1 vs 32.3 ± 9.8 HU; $p = 0.58$).

At delayed enhancement DECT (40-keV level), a signal attenuation higher than 161 HU had a sensitivity of 65% and a specificity of 80% for the identification of MI using SPECT as the reference standard and of 72% and 79%, respectively, using combined SPECT and perfusion CT as the reference standard.

Good intraobserver reproducibility was observed regarding the signal attenuation of segments with MI (ICC, 0.99; $p < 0.0001$) and of remote normal myocardium (ICC, 0.98; $p < 0.0001$).

Detection of Myocardial Infarction Using Perfusion CT Compared With Delayed Enhancement Dual-Energy CT

On a per-territory basis, the sensitivity, specificity, PPV, and NPV of perfusion CT for the identification of MI were 92.9% (95% CI, 66–100%), 96.6% (95% CI, 90–99%), 81.3% (95% CI, 54–96%), and 98.8% (95% CI, 94–100%), whereas delayed enhancement DECT had a sensitivity, specificity, PPV, and NPV of 85.7% (95% CI, 57–98%), 96.6% (95% CI, 90–99%), 80.0% (95% CI, 52–96%), and 97.7% (95% CI, 92–100%), respectively. The AUC under the ROC curve for the identification of MI was similar for perfusion CT and delayed enhancement DECT on a per-territory basis (AUC, 0.95 [95% CI, 0.88–0.98] vs 0.91 [95% CI, 0.84–0.96]; $p = 0.58$). Further diagnostic performance results on a per-patient basis and per-segment basis are provided in Table 3.

Paired Comparison Between Energy Levels Using Delayed Enhancement Dual-Energy CT

Differences regarding signal attenuation and image noise between segments with MI identified by both perfusion CT and SPECT and same-slice remote (normal perfusion) myocardium were significantly higher among low energy levels (Figs. 2 and 3) and were progressively declining at increasing energy levels (40 keV = 221.2 ± 57.5 HU vs 141.3 ± 24.7 HU, $p < 0.0001$; 140 keV = 45.4 ± 8.2 HU vs 35.6 ± 7.5 HU, $p = 0.03$). The median (interquartile range) signal attenuation of segments with MI was more than 2 SDs above the mean signal attenuation of the normal myocardium among low energy levels (40 keV = 3.0 SDs [1.3–4.0 SDs]; 60 keV = 2.7 SDs [0.9–5.8 SDs]; 80 keV = 1.9 SDs [0.8–4.1 SDs]; 100 keV = 1.3 SDs [0.6–4.0 SDs]; 120 keV = 1.2 SDs [0–3.7 SDs]; 140 keV = 1.1 SDs [–0.2 to 3.3 SDs], $p < 0.0001$). At 40 keV, only one (7%) myocardial infarct showed a signal attenuation more than 6 SDs higher than that of the remote normal myocardium. Furthermore, differences between left ventricular blood pool signal attenuation and myocardial (infarction vs remote normal) signal attenuation were significantly higher at low energy levels (Table 4).

Image noise of both segments with MI (40 keV = 57.8 ± 28.0 HU, 60 keV = 26.3 ± 12.0 HU, 80 keV = 16.3 ± 6.6 HU, 100 keV = 14.9 ± 5.6 HU, 120 keV = 13.1 ± 4.6 HU, 140 keV = 12.0 ± 4.1 HU; $p < 0.0001$) and remote normal myocardium (40 keV = 52.9 ± 22.6 HU, 60 keV = 23.9 ± 10.3 HU, 80 keV = 14.4 ± 5.2 HU, 100 keV = 13.8 ± 5.0 HU, 120 keV = 11.9 ± 4.2 HU, 140 keV = 11.2 ± 3.6 HU; $p < 0.0001$) was significantly higher at lower energy levels.

Finally, delayed DECT images of two patients showed evidence of lipomatous meta-

TABLE 3: Diagnostic Performance of Perfusion CT and Delayed Enhancement Dual-Energy CT (DECT) for the Detection of Myocardial Infarction When SPECT Was Used as the Reference Standard

Performance Value	Perfusion CT	Delayed Enhancement DECT	*p*
Per patient			
Sensitivity (%)	92.3 (64–100)	92.3 (64–100)	
Specificity (%)	85.7 (64–97)	90.5 (70–99)	
PPV (%)	80.0 (52–96)	85.7 (57–98)	
NPV (%)	94.7 (74–100)	95.0 (75–100)	
Area under ROC curve	0.89 (0.74–0.97)	0.91 (0.77–0.98)	0.70
Per territory			
Sensitivity (%)	92.9 (66–100)	85.7 (57–98)	
Specificity (%)	96.6 (90–99)	96.6 (90–99)	
PPV (%)	81.3 (54–96)	80.0 (52–96)	
NPV (%)	98.8 (94–100)	97.7 (92–100)	
Area under ROC curve	0.95 (0.88–0.98)	0.91 (0.84–0.96)	0.58
Per segment			
Sensitivity (%)	78.6 (67–87)	55.7 (43–68)	
Specificity (%)	95.4 (93–97)	96.8 (95–98)	
PPV (%)	71.4 (60–81)	72.2 (58–84)	
NPV (%)	96.8 (95–98)	93.7 (91–96)	
Area under ROC curve	0.87 (0.84–0.90)	0.76 (0.73–0.80)	0.0006

Note—The values in parentheses are 95% CIs. PPV = positive predictive value, NPV = negative predictive value.

TABLE 4: Signal Attenuation and Signal-to-Noise Ratio of Myocardial Infarction (MI) and Remote Normal Myocardial Segments Among the Energy Levels in the Spectrum Using Delayed Enhancement Dual-Energy CT

Parameter	Energy Level (keV)					
	40	60	80	100	120	140
Signal attenuation (HU)						
MI	221.2 ± 57.5	120.5 ± 41.0	76.1 ± 15.4	59.1 ± 11.8	49.3 ± 10.1	45.4 ± 8.2
Remote myocardium	141.3 ± 24.7	83.7 ± 10.9	54.1 ± 10.1	43.7 ± 7.3	37.6 ± 6.6	35.6 ± 7.5
p	< 0.0001	0.004	0.001	0.005	0.02	0.03
LV–MI segment ratio	1.05 ± 0.1	1.08 ± 0.3	1.01 ± 0.1	0.99 ± 0.1	0.99 ± 0.1	0.97 ± 0.1
LV–remote myocardium ratio	1.62 ± 0.2	1.47 ± 0.3	1.46 ± 0.4	1.38 ± 0.4	1.35 ± 0.5	1.32 ± 0.5
p	< 0.0001	0.009	0.002	0.008	0.02	0.04
Signal-to-noise ratio						
MI	5.10 ± 3.1	5.71 ± 3.5	5.63 ± 3.1	4.68 ± 2.3	4.37 ± 2.2	4.39 ± 2.1
Remote myocardium	3.31 ± 1.8	4.34 ± 2.3	4.47 ± 2.5	3.65 ± 1.7	3.60 ± 1.7	3.62 ± 1.9
p	0.004	0.07	0.17	0.14	0.30	0.29

Note—Results are reported as mean ± SD. LV = left ventricle.

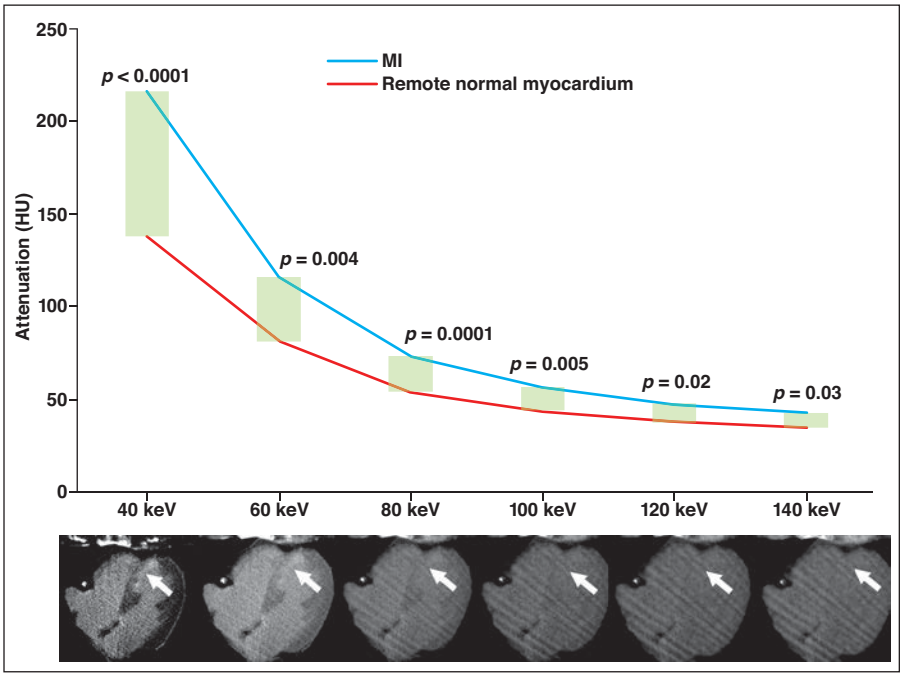

Fig. 3—Delayed enhancement dual-energy CT (DECT) images of 68-year-old man obtained at increasing energy levels show myocardial infarct at septal wall (*arrows*), better depicted at lowest energy levels. Above DECT images, graph shows signal attenuation levels (in Hounsfield units) of segments with myocardial infarction (MI) on both perfusion CT and SPECT (scar) compared with signal attenuation of remote (normal) myocardium. Shaded areas in graph show attenuation difference between MI and normal myocardium at different energy levels.

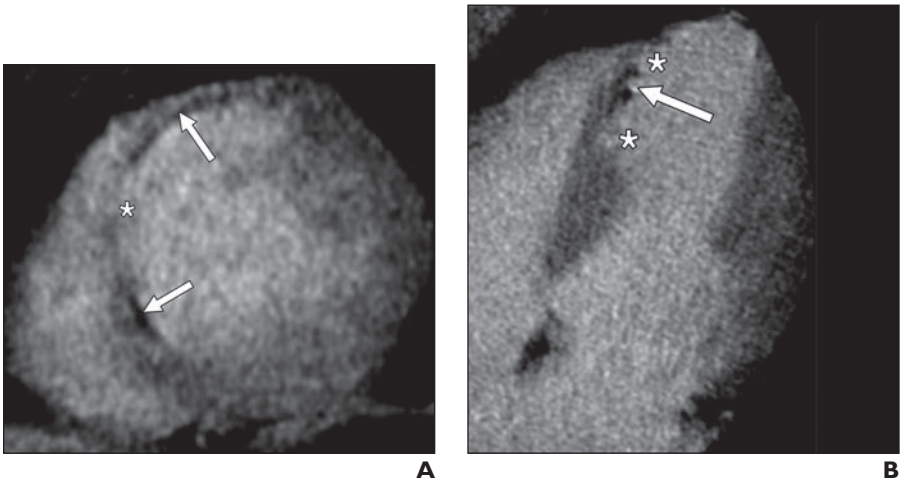

Fig. 4—52-year-old man (body mass index [weight in kilograms divided by the square of height in meters], 30.4) with history of myocardial infarction.
A and **B,** Virtual monochromatic reconstruction delayed enhancement dual-energy CT images obtained at 40 keV show areas of lipomatous metaplasia (*arrows*) and late iodine enhancement at septal and anterior mid and apical left ventricular wall (*asterisks*).

(Fig. 4 continues on next page)

Downloaded from www.ajronline.org by Lund University Medicinska Fakultetens Bibl. on 09/02/17 from IP address 130.235.66.10. Copyright ARRS. For personal use only; all rights reserved

Downloaded from www.ajronline.org by Lund University Medicinska Fakultetens Bibl. on 09/02/17 from IP address 130.235.66.10. Copyright ARRS. For personal use only; all rights reserved

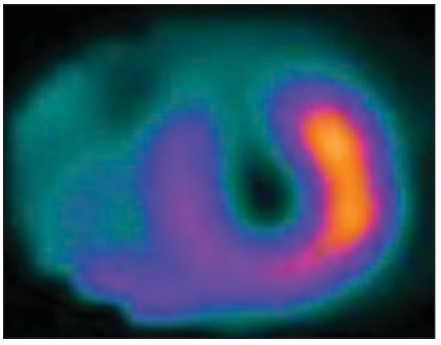

C

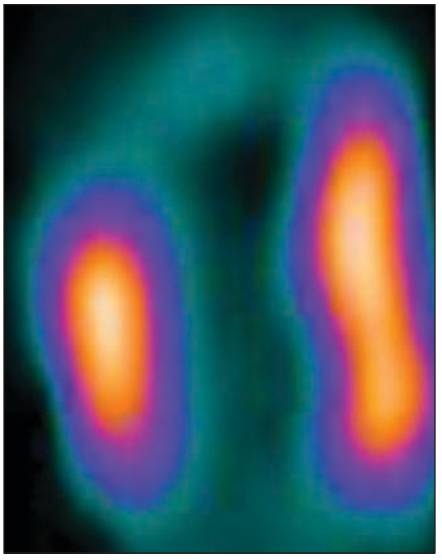

D

Fig. 4 (continued)—52-year-old man (body mass index [weight in kilograms divided by the square of height in meters], 30.4) with history of myocardial infarction.
C and **D,** Rest SPECT images confirm absence of radiotracer uptake in same segments.

plasia, and there was no evidence of late iodine enhancement over segments with adipose tissue infiltration (Fig. 4). Delayed DECT images of both patients also showed concomitant areas of late enhancement.

Discussion

The main finding of our study was that VMI at low energy levels derived from delayed enhancement DECT allowed the detection of myocardial infarcts; our results showed that a signal attenuation threshold of more than 2 SDs above the mean attenuation of normal myocardium might be a reasonable cutoff value for infarct detection in a stable setting.

Delayed enhancement DECT has earned interest in the past years as an adjunct to perfusion CT protocols including rest and stress perfusion CT [4, 5]. Nonetheless, although delayed enhancement CT performed using conventional single-energy scanners has reasonable contrast resolution in patients with acute MI, the diagnostic performance of conventional delayed enhancement DECT for the detection of chronic infarcts is only moderate mainly because of suboptimal tissue contrast, with excellent specificity but low sensitivity (only 50–60% of patients with late gadolinium enhancement at cardiac MRI detected) [2, 4, 6, 18]. In a previous study of Bettencourt et al. [4], this suboptimal tissue contrast has led to a lack of improvement of delayed enhancement DECT over the global accuracy of cardiac CT for the detection of hemodynamically significant lesions in patients at intermediate to high probability of CAD [4]. Similar discouraging findings have been reported using dual-source CT scanners [5].

Despite the aforementioned shared contrast kinetics of gadolinium and iodine, delayed enhancement MRI achieves significantly higher contrast between scar and remote normal myocardium, at least partly because of the ability of cardiac MRI to null the normal myocardium using specific inversion times. On the contrary, delayed enhancement DECT has a significantly lower contrast-to-noise ratio compared with delayed enhancement MRI; thus, on conventional delayed enhancement CT, scarred areas are typically depicted as segments where the discrimination between myocardium and the left ventricular blood pool is unclear [8].

To our knowledge, our study is the first to explore the ability of VMI using delayed enhancement DECT from single-source rapid-kilovoltage-switching dual-energy imaging to discriminate between myocardial infarcts and remote normal myocardium, with our results showing a clear distinction between these tissues. Previously, Meinel et al. [19] reported a lack of incremental value of delayed enhancement DECT over rest-stress perfusion CT using dual-energy imaging from a dual-source CT scanner.

In our study, the largest differences between scarred and remote normal segments were observed at the lowest energy levels, which typically show the highest attenuation levels. Importantly, the signal attenuation of the scarred areas was 3 SDs above that of the normal myocardium, although only 7% of myocardial infarcts showed a signal attenuation higher than 6 SDs. This is an obvious advantage of delayed enhancement MRI over delayed enhancement DECT, although it is particularly useful for quantitative analysis [20] and not for qualitative analysis as in our study.

The highest signal attenuation levels observed at 40 keV were attained at detriment of a significantly higher image noise. This limitation is expected to be partially mitigated by the recent developments in iterative reconstruction algorithms for energy levels below 60 keV. Our results might add to the increasing evidence supporting the role of delayed enhancement DECT as a safe (i.e., associated with low radiation dose) and potentially time-saving and cost-saving alternative for myocardial scar detection among patients with contraindications to delayed enhancement MRI. Delayed enhancement DECT might potentially be particularly useful for imaging patients with claustrophobia, implantable cardiac devices, or impaired breath-holding capabilities. Indeed, recent concerns, even if overemphasized, regarding delayed enhancement cardiac MRI safety, including reports of DNA double-strand breaks and gadolinium-associated nephrogenic systemic fibrosis and deposition in the skin and brain, might encourage the role of delayed enhancement DECT as an alternative for delayed enhancement MRI in selected patients [21–23].

Further studies are warranted exploring whether delayed enhancement DECT using VMI might potentially offer improved sensitivity compared with conventional delayed enhancement single-energy CT [4].

In keeping with the results from previous studies including chronic myocardial infarcts [7, 24], segments with lipomatous metaplasia did not show delayed enhancement in our study.

In our study, the diagnostic performance of delayed enhancement DECT for the detection of myocardial infarcts was high on a per-patient basis and per-territory basis but was fairly low on a per-segment basis. These findings might suggest that delayed enhancement DECT appears as a highly specific but moderately sensitive means to identify scar tissue. Alternatively, this discrepancy might possibly be related to the coexistence of an admixture of necrotic and viable myocardium, although this cannot be fully elucidated without cardiac MRI or PET.

Overall, the addition of delayed scanning might not offer a significant incremental di-

Downloaded from www.ajronline.org by Lund University Medicinska Fakultetens Bibl. on 09/02/17 from IP address 130.235.66.10. Copyright ARRS. For personal use only; all rights reserved

agnostic value in the context of stress-rest cardiac CT. Nonetheless, we provide proof of concept for scar imaging using VMI derived from delayed enhancement DECT and establish threshold levels for scar tissue detection. The use of delayed enhancement DECT as an add-on diagnostic tool among patients undergoing coronary CT angiography might potentially have a relevant clinical impact because it has been previously shown that the presence of unrecognized non–Q-wave MI is a predictor of mortality in patients with suspected coronary disease [25]. Indeed, in a recent study involving survivors of sudden cardiac arrest, 44% of the patients had unrecognized myocardial infarcts [26].

Furthermore, our results should encourage the exploration of delayed enhancement DECT using VMI as an alternative for scar imaging in patients with nonischemic cardiomyopathies. In this regard, a number of studies have reported promising findings particularly among patients with hypertrophic cardiomyopathy, whereas emerging data suggest a role of delayed enhancement DECT in patients with myocarditis as well as a tool to aid myocardial scar detection toward electroanatomic mapping [7, 27–29].

With regard to radiation safety issues, we reported a mean effective radiation dose of 2.2 mSv associated with delayed enhancement DECT using VMI. This dose, albeit lower than the overall annual nonmedical effective dose radiation per capita (3 mSv), was higher than the previously reported dose using low-tube-voltage (80-kV) imaging, but it is significantly lower than the radiation dose reported using DECT derived from dual-source scanners [4, 19, 30, 31].

A number of limitations should be acknowledged. The relatively small number of patients might influence the results because of the potential for selection bias. Furthermore, diagnostic performance results might be influenced by the fact that SPECT lacks the sufficient spatial resolution (compared with delayed enhancement cardiac MRI or PET) to be used as an accurate reference standard for scar imaging. Nonetheless, SPECT has been previously validated as an accurate tool to assess the presence and extension of MI [32]. This limitation might be attenuated using the combined findings of SPECT and perfusion CT as the reference standard, and the diagnosis of MI was supported by clinical history and ECG findings. Finally, reliable data regarding infarct age were not available, and iodine maps were not obtained because the aim of the study was to assess VMI derived from DECT.

Conclusion

In this pilot study, delayed enhancement DECT at low energy levels allowed the detection of myocardial infarcts in the stable setting. Further studies are warranted to explore whether this technique might become an alternative for scar imaging in patients not suitable for cardiac MRI.

References

1. Gerber BL, Belge B, Legros GJ, et al. Characterization of acute and chronic myocardial infarcts by multidetector computed tomography: comparison with contrast-enhanced magnetic resonance. *Circulation* 2006; 113:823–833
2. Nieman K, Shapiro MD, Ferencik M, et al. Reperfused myocardial infarction: contrast-enhanced 64-section CT in comparison to MR imaging. *Radiology* 2008; 247:49–56
3. Lardo AC, Cordeiro MA, Silva C, et al. Contrast-enhanced multidetector computed tomography viability imaging after myocardial infarction: characterization of myocyte death, microvascular obstruction, and chronic scar. *Circulation* 2006; 113:394–404
4. Bettencourt N, Ferreira ND, Leite D, et al. CAD detection in patients with intermediate-high pretest probability: low-dose CT delayed enhancement detects ischemic myocardial scar with moderate accuracy but does not improve performance of a stress-rest CT perfusion protocol. *JACC Cardiovasc Imaging* 2013; 6:1062–1071
5. Blankstein R, Shturman LD, Rogers IS, et al. Adenosine-induced stress myocardial perfusion imaging using dual-source cardiac computed tomography. *J Am Coll Cardiol* 2009; 54:1072–1084
6. Rodriguez-Granillo GA, Rosales MA, Baum S, et al. Early assessment of myocardial viability by the use of delayed enhancement computed tomography after primary percutaneous coronary intervention. *JACC Cardiovasc Imaging* 2009; 2:1072–1081
7. Esposito A, Palmisano A, Antunes S, et al. Cardiac CT with delayed enhancement in the characterization of ventricular tachycardia structural substrate: relationship between CT-segmented scar and electro-anatomic mapping. *JACC Cardiovasc Imaging* 2016; 9:822–832
8. Goetti R, Feuchtner G, Stolzmann P, et al. Delayed enhancement imaging of myocardial viability: low-dose high-pitch CT versus MRI. *Eur Radiol* 2011; 21:2091–2099
9. Carrascosa PM, Deviggiano A, Capunay C, et al. Incremental value of myocardial perfusion over coronary angiography by spectral computed tomography in patients with intermediate to high likelihood of coronary artery disease. *Eur J Radiol* 2015; 84:637–642
10. Carrascosa P, Capunay C, Rodriguez-Granillo GA, Deviggiano A, Vallejos J, Leipsic JA. Substantial iodine volume load reduction in CT angiography with dual-energy imaging: insights from a pilot randomized study. *Int J Cardiovasc Imaging* 2014; 30:1613–1620
11. Carrascosa P, Leipsic JA, Capunay C, et al. Monochromatic image reconstruction by dual energy imaging allows half iodine load computed tomography coronary angiography. *Eur J Radiol* 2015; 84:1915–1920
12. Henzlova MJ, Duvall WL, Einstein AJ, Travin MI, Verberne HJ. ASNC imaging guidelines for SPECT nuclear cardiology procedures: stress, protocols, and tracers. *J Nucl Cardiol* 2016; 23:606–639
13. Cerqueira MD, Weissman NJ, Dilsizian V, et al. Standardized myocardial segmentation and nomenclature for tomographic imaging of the heart: a statement for healthcare professionals from the Cardiac Imaging Committee of the Council on Clinical Cardiology of the American Heart Association. *Circulation* 2002; 105:539–542
14. Hachamovitch R, Berman DS, Kiat H, et al. Exercise myocardial perfusion SPECT in patients without known coronary artery disease: incremental prognostic value and use in risk stratification. *Circulation* 1996; 93:905–914
15. Arruda-Olson AM, Roger VL, Jaffe AS, Hodge DO, Gibbons RJ, Miller TD. Troponin T levels and infarct size by SPECT myocardial perfusion imaging. *JACC Cardiovasc Imaging* 2011; 4:523–533
16. Halliburton SS, Abbara S, Chen MY, et al.; Society of Cardiovascular Computed Tomography. SCCT guidelines on radiation dose and dose-optimization strategies in cardiovascular CT. *J Cardiovasc Comput Tomogr* 2011; 5:198–224
17. DeLong ER, DeLong DM, Clarke-Pearson DL. Comparing the areas under two or more correlated receiver operating characteristic curves: a nonparametric approach. *Biometrics* 1988; 44:837–845
18. Boussel L, Ribagnac M, Bonnefoy E, et al. Assessment of acute myocardial infarction using MDCT after percutaneous coronary intervention: comparison with MRI. *AJR* 2008; 191:441–447
19. Meinel FG, De Cecco CN, Schoepf UJ, et al. First-arterial-pass dual-energy CT for assessment of myocardial blood supply: do we need rest, stress, and delayed acquisition? Comparison with SPECT. *Radiology* 2014; 270:708–716
20. Schulz-Menger J, Bluemke DA, Bremerich J, et al. Standardized image interpretation and post processing in cardiovascular magnetic resonance: Society for Cardiovascular Magnetic Resonance (SCMR) board of trustees task force on standardized post processing. *J Cardiovasc Magn Reson* 2013; 15:35
21. Lancellotti P, Nchimi A, Delierneux C, et al. Bio-

logical effects of cardiac magnetic resonance on human blood cells. *Circ Cardiovasc Imaging* 2015; 8:e003697

22. Stojanov D, Aracki-Trenkic A, Benedeto-Stojanov D. Gadolinium deposition within the dentate nucleus and globus pallidus after repeated administrations of gadolinium-based contrast agents: current status. *Neuroradiology* 2016; 58:433–441
23. Roberts DR, Lindhorst SM, Welsh CT, et al. High levels of gadolinium deposition in the skin of a patient with normal renal function. *Invest Radiol* 2016; 51:280–289
24. Arnold JR, Karamitsos TD, Pegg TJ, Francis JM, Neubauer S. Left ventricular lipomatous metaplasia following myocardial infarction. *Int J Cardiol* 2009; 137:e11–e12
25. Kim HW, Klem I, Shah DJ, et al. Unrecognized non-Q-wave myocardial infarction: prevalence and prognostic significance in patients with suspected coronary disease. *PLoS Med* 2009; 6:e1000057
26. Neilan TG, Farhad H, Mayrhofer T, et al. Late gadolinium enhancement among survivors of sudden cardiac arrest. *JACC Cardiovasc Imaging* 2015; 8:414–423
27. Shiozaki AA, Senra T, Arteaga E, et al. Myocardial fibrosis detected by cardiac CT predicts ventricular fibrillation/ventricular tachycardia events in patients with hypertrophic cardiomyopathy. *J Cardiovasc Comput Tomogr* 2013; 7:173–181
28. Zhao L, Ma X, Delano MC, et al. Assessment of myocardial fibrosis and coronary arteries in hypertrophic cardiomyopathy using combined arterial and delayed enhanced CT: comparison with MR and coronary angiography. *Eur Radiol* 2013; 23:1034–1043
29. Axsom K, Lin F, Weinsaft JW, Min JK. Evaluation of myocarditis with delayed-enhancement computed tomography. *J Cardiovasc Comput Tomogr* 2009; 3:409–411
30. Wang R, Zhang Z, Xu L, et al. Low dose prospective ECG-gated delayed enhanced dual-source computed tomography in reperfused acute myocardial infarction comparison with cardiac magnetic resonance. *Eur J Radiol* 2011; 80:326–330
31. Einstein AJ. Effects of radiation exposure from cardiac imaging: how good are the data? *J Am Coll Cardiol* 2012; 59:553–565
32. Slomka PJ, Fieno D, Thomson L, et al. Automatic detection and size quantification of infarcts by myocardial perfusion SPECT: clinical validation by delayed-enhancement MRI. *J Nucl Med* 2005; 46:728–735

Downloaded from www.ajronline.org by Lund University Medicinska Fakultetens Bibl. on 09/02/17 from IP address 130.235.66.10. Copyright ARRS. For personal use only; all rights reserved